Electronic Supplementary Material (ESI) for Nanoscale.
This journal is © The Royal Society of Chemistry 2020

Supplementary information

DNA-directed arrangement of soft synthetic compartments and their behavior *in vitro* and *in vivo*

Juan Liu[†,†], Ioana Craciun[†,†], Andrea Belluati[†], Dalin Wu[†], Sandro Sieber[‡], Tomaz Einfalt[‡], Dominik Witzigmann[‡], Mohamed Chami[§], Jörg Huwyler[‡] and Cornelia G. Palivan[†]*

[†]Department of Chemistry, University of Basel, Mattenstrasse 24a, Basel-4058, Switzerland, [‡]Division of Pharmaceutical Technology, Department of Pharmaceutical Sciences, University of Basel, Klingelbergstrasse 50, Basel-4056, Switzerland, [§]BioEM lab, Biozentrum, University of Basel, Mattenstrasse 26, Basel-4058, Switzerland

[†]J.L. and I.C. contributed equally to this work.

*Corresponding author: Cornelia G. Palivan
Email address: cornelia.palivan@unibas.ch
Phone number: +41 612073839

Supplementary methods

Formation of ssDNA-polymersomes. Poly(dimethylsiloxane)-*block*-poly(2-methyloxazoline) ($PDMS_{62}$-$PMOXA_{13}$) alone self-assembles to polymersomes with an apparent hydrodynamic diameter (D_H) of 200 ± 30 nm while azide-functionalized polymer $PDMS_{71}$-$PMOXA_{25}$-OEG_3-N_3 alone forms spherical micelles (Figure S2A, H). Therefore, the azide terminated polymer can interfere with the self-assembly of the diblock copolymer resulting in not only polymersomes but also other assembled structures. We started by preparing mixtures of $PDMS_{62}$-$PMOXA_{13}$ with increasing concentrations of $PDMS_{71}$-$PMOXA_{25}$-OEG_3-N_3 and were able to increase the content of $PDMS_{71}$-$PMOXA_{25}$-OEG_3-N_3 up to 20 mol% without perturbing the self-assembly process or the resulting apparent D_H of the polymersomes (Figure S2B-F and Table S2). When increasing the content of $PDMS_{71}$-$PMOXA_{25}$-OEG_3-N_3 to 33 mol%, a low population of worm-like micelles appeared (Figure 2G), indicating that a limit for the tolerance of the azide-functionalized polymer was reached. Using these two polymers, we were able to increase the maximal content of azide-functionalized polymer incorporated into the polymersomes, which we assume was due to the low hydrophobic mismatch.

Next, we linked DBCO-ssDNA to polymersomes bearing azide-functional groups and aimed at regulating the number of ssDNA per polymersome. Prior to linking DBCO-ssDNA to polymersomes, the availability of azide groups on the polymersome's surface was probed by conjugation with DBCO- OEG_4-ATTO 488 and the number of azide groups per polymersome was evaluated by fluorescence correlation spectroscopy (FCS). FCS is a correlation analysis of temporal fluctuations of the fluorescence intensity and offers insights, among other parameters, into the diffusion behavior of fluorescent subjects and their average brightness per molecule (count per molecules, CPM). The number of azide groups per polymersome was calculated by dividing

the CPM of DBCO-OEG_4-ATTO 488 conjugating polymersomes with the one of DBCO-OEG_4-ATTO 488. The increase in diffusion time (τ_D) from 38.1 ± 7.5 µs for free DBCO-OEG_4-ATTO 488 in solution to 2.7 ± 0.6 ms – 4.0 ± 0.8 ms for 488-conjuagted polymersomes confirms the presence and the availability of azide groups on the polymersome's surface (Figure S3A). The number of azide groups per polymersome was determined to range from 19 ± 9 to 592 ± 111 as the molar fraction of $PDMS_{71}$-$PMOXA_{25}$-OEG_3-N_3 was varied from 0.5 mol% to 33 mol% (Figure S3B). After confirming the number of azide groups per polymersome, we linked DBCO-ssDNAa with their 3' ends labelled with ATTO 488 (ssDNAa-ATTO 488) and the complementary DBCO-ssDNAb labeled with Cy5 (ssDNAb-Cy5), to distinct polymersomes (Figure 1A). The increase in the τ_D of ssDNAa-ATTO 488 (128.8 ± 7.9 µs) and ssDNAb-Cy5 (64.3 ± 8.3 µs) to ssDNAa-ATTO 488 conjugated polymersomes (2.3 ± 1.4 ms – 5.6 ± 1.1 ms) and ssDNAb-Cy5 conjugated ones (1.9 ± 3.7 ms - 9.1 ± 2.8 ms) confirmed that the ssDNAs were linked to the polymersomes (Figure S3C, 3D). The number of ssDNAa-ATTO 488 and ssDNAb-Cy5 per polymersome is in the range of 9 ± 9 to 289 ± 72 and 1 ± 1 to 156 ± 18, respectively (Figure S3B), but more importantly the ssDNA conjugation did not alter the morphology of distinct polymersomes (Figure S1I-N and Table S2). As expected, the number of linked ssDNAs per polymersome was lower as compared to linked dye molecules, since the molecular weight of ssDNA is considerably larger than DBCO-ATTO 488, resulting in steric hindrance.

Analytical methods

Nuclear magnetic resonance (NMR) spectroscopy. ^1H NMR spectra were recorded on a Bruker DPX-400 MHz spectrometer in $CDCl_3$ without tetramethylsilane standard and analyzed using MestReNova software (Mestrelab Research S.L., Spain). All spectra were aligned to the

chemical shift of $CDCl_3$ at 7.26 ppm. The block ratio and number-average molecular weight of block copolymers was determined by ^1H NMR end-group analysis.

Gel permeation chromatography (GPC). GPC traces were recorded and analyzed in WinGPC UniCrom (V 8.20 - build 4815, Polymer Standard Service (PSS), Germany). The TCM GPC system was equipped with a series of linear-S SDV columns (pre-column (5 cm), three analytical columns (30 cm), all 5 μm particles and 0.8 cm in diameter, PSS, Germany) or a pair of SDV columns (pre-column (5 cm), a 103 Å and a 105 Å both 30 cm, all 5 μm particles and 0.8 cm in diameter, PSS, Germany) and detector system including VWD (1100 series), RI (1100 series) and a viscometer (PSS DVD1260). Detector and columns were kept at 35 °C using TCM, stabilized with EtOH, as the eluent at a flow rate of 1 mL min^{-1}.

Dynamic light scattering (DLS). The measurements of apparent D_H of polymersomes, ssDNA-polymersomes and polymersome clusters were performed on a Zetasizer Nano ZSP (Malvern Instruments, UKl) at 25 °C. 400 μL of 0.2 mg/mL (final concentration) of either polymersomes or polymersome clusters were added to a cuvette and measured during 11 runs repeated three times. The measured angle was 173° and the data was analyzed by number distribution. For the kinetics of polymersome cluster formation, each measurement was run for 3 mins with 2 mins interval.

Transmission electron microscopy (TEM). A 5 μL of polymersomes or polymersome clusters (0.1 mg/mL) was absorbed on copper grids with 400 mesh square. The grids were further stained with 2% uranyl acetate and the negatively stained image of nanostructures was performed on a transmission electron microscope (Philips CM100) at an acceleration voltage of 80 kV.

Cryogenic transmission electron microcopy (CryoTEM). A 4 μL of polymersome clusters (0.2 mg/mL) was adsorbed on a holey carbon-coated grid (Quantifoil, Germany), blotted with a

Whatman 1 filter paper and vitrified in liquid nitrogen-cooled liquid ethane using an FEIVitrobot MK4 (FEI Company, The Netherlands). Frozen grids were transferred to a Philips CM200-FEG electron microscope, which was operated at an acceleration voltage of 200 kV. Digital electron micrographs were recorded with a 4k × 4k TemCam-F416 CMOS camera (TVIPS Company, Germany).

Confocal laser scanning microscopy (CLSM). CLSM measurements were recorded on a confocal laser scanning microscope (ZEISS LSM 880, inverted microscope ZEISS Axio Observer, Carl Zeiss, Germany). In general, 20 μL of 0.1 mg/mL of polymersome or polymersome clusters were dropped and immobilized on an amino-functionalized glass slide[1] by the electrostatic attraction between ssDNA and amino groups on the surface for the measurements. For visualizing either single polymersomes or polymersome clusters, three lasers, 488 nm of an argon laser, 561 nm of DPSS 5561-10 laser and 633 nm of HeNe laser, were used. For the clusters assembled by DY-633-P20-a and ATTO 488-P20-b and their *in vitro* studies, 488 nm argon laser and 633 nm HeNe laser were passed through MBS488 and MBS488/561/633 filters before focusing the beam through a water immersion objective (C-Apochromate 40x/1.2W korr FCS M27) onto the sample and detected in the range of 505-555 nm and 650-740 nm, respectively. For the clusters assembled by DY-633-P20-a and SRB-P20-b that was used for *in vivo* studies, DPSS 5561-10 laser and HeNe laser were passed through MBS 488/561 and MBS 488/561/633 filters and detected in the range of 578 nm-620 nm and 650-740 nm, respectively.

Fluorescence Correlation Spectroscopy (FCS). FCS was performed on a Zeiss LSM 880 microscope (Zeiss LSM 880, inverted microscope ZEISS Axio Observer, Carl Zeiss, Jena, Germany) with adjusted settings from above: 488nm argon laser were used to excite ssDNAa-ATTO 488 and the conjugated polymersomes and 633 nm HeNe laser was exploited for ssDNAb-

Cy5 and the conjugated polymersomes. The two lasers were passed through MBS488 and MBS488/561/633 filters and the signals were detected in the range of 500-532 nm and 657-690 nm, respectively. The pinholes were adjusted to maximize the count rate using the respective free dye in PBS and the sample volumes were 15 µL. Fluorescent fluctuations over time were recorded for 30 x 10 s. The raw data was processed and analyzed using Zeiss software. Autocorrelation curves were fitted by a two-component model (Supplementary Equation 1).

$$G_{2comp}(\tau) = 1 + \frac{1}{N} \cdot \left(1 + \frac{T_{trip}}{1 - T_{trip}} e^{-\frac{\tau}{\tau_{trip}}}\right) \cdot \left[\frac{f_1}{\left(1 + \frac{\tau}{\tau_{D_1}}\right)\left(1 + \frac{\tau}{S^2\tau_{D_1}}\right)^{1/2}} + \frac{f_2}{\left(1 + \frac{\tau}{\tau_{D_2}}\right)\left(1 + \frac{\tau}{S^2\tau_{D_2}}\right)^{1/2}}\right]$$

(1)

Where $G_{2comp}(\tau)$ is the two-component autocorrelation function, *N* is the number of particles, S the structural parameter, T_{trip} is the fraction of fluorophores in the triplet state, τ_{trip} is the corresponding triplet time, f_1 and f_2 are the fraction of the particles of the corresponding component 1 or 2, τ_{D_1} and τ_{D_2} are the diffusion times of the corresponding component 1 or 2.

UV-Vis spectroscopy. UV-vis absorbance of 800 µL of non-encapsulated free ATTO 488, DY-633 and SRB were measured on a Thermo Scientific NanoDrop 2000c UV−Vis spectrophotometer (Thermo Fisher Scientific, Waltham, MA, USA) equipped with a xenon flash lamp using 1 cm path-length quartz cuvettes (Hellma, QS).

ζ-potential analysis. The ζ-potential of the ssDNA-polymersomes and polymersome clusters in PBS and cell medium with serum was determined by measuring the direction and velocity of polymersome movement in an applied electrical field using the Zetasizer Nano ZSP (Malvern

Instruments, UK). 800 μL of a 0.1 mg/mL polymersome solution was used and the results were reported as mean values obtained from three measurements.

Statistical analysis

A. Statistical analysis of the apparent size distribution of the DNA-linked polymersome clusters was fitted with lognormal distribution functions:

(a) P1-a (Figure S4B)

#Parameters:

	estimate	Std. Error
#shape	0.8177468	0.3332769
#rate	7.3598622	4.0444157

#One-sample Kolmogorov-Smirnov test

D = 0.23589, p-value = 0.6181

(a) P1-ab (Figure S4B)

#Parameters:

	estimate	Std. Error
#shape	1.242265	0.4549012
#rate	14.907928	6.6865770

One-sample Kolmogorov-Smirnov test

D = 0.16923, p-value = 0.8271

(b) P5-a (Figure S4C)

#Parameters:

	estimate	Std. Error
#shape	1.618134	0.6624725

(b) P5-ab (Figure S4C)

#Parameters:

	estimate	Std. Error
#shape	1.213947	0.4107746

#rate 16.182874 7.7511100

One-sample Kolmogorov-Smirnov test

D = 0.17228, p-value = 0.8807

#rate 16.996332 7.0762851

One-sample Kolmogorov-Smirnov test

D = 0.19036, p-value = 0.6241

(c) P10-a (Figure S4D)

#Parameters:

estimate Std. Error

#shape 1.788555 0.8244338

#rate 14.307910 7.6029187

One-sample Kolmogorov-Smirnov test

D = 0.2076, p-value = 0.8162

(b) P10-ab (Figure S4D)

#Parameters:

estimate Std. Error

#shape 1.313109 0.464061

#rate 17.072865 7.313026

One-sample Kolmogorov-Smirnov test

D = 0.17488, p-value = 0.7606

(d) P20-a (Figure 1d, Figure S4E)

#Parameters:

estimate Std. Error

#shape 1.322201 0.4866227

#rate 15.868394 7.0695371

(d) P20-ab (Figure 1d, Figure S4E)

#Parameters:

estimate Std. Error

#shape 1.034356 0.3133142

#rate 17.585299 6.7794168

One-sample Kolmogorov-Smirnov test

D = 0.18543, p-value = 0.7389

One-sample Kolmogorov-Smirnov test

D = 0.15771, p-value = 0.7347

B. Statistical analysis of the distribution of the number of polymersomes per cluster was obtained by using a lognormal distribution function:

(a) P1-ab (Figure S4B)

#Parameters:

estimate Std. Error

#shape 0.2244392 0.07078994

#rate 2.6921829 1.84719446

One-sample Kolmogorov-Smirnov test

D = 0.21047, p-value = 0.6624

(b) P5-ab (Figure S4C)

#Parameters:

estimate Std. Error

#shape 0.3566462 0.1009897

#rate 5.7055319 2.8835590

One-sample Kolmogorov-Smirnov test

D = 0.24809, p-value = 0.2783

(c) P10-ab (Figure S4D)

#Parameters:

estimate Std. Error

#shape 0.2897568 0.1020283

#rate 2.8982581 1.9850496

One-sample Kolmogorov-Smirnov test

D = 0.3215, p-value = 0.2525

(d) P20-ab (Figure S4E)

#Parameters:

estimate Std. Error

#shape 0.205505 0.05965282

#rate 2.878460 1.89155503

One-sample Kolmogorov-Smirnov test

D = 0.20645, p-value = 0.5895

C. The statistical analysis of the co-localization data of DY-633-P20-a and SRB-P20-b polymersomes and associated DNA-linked polymersome clusters, was performed using OriginPro 9.1 software (OriginLab Corporation; Northampton, MA). Statistical significance was calculated based on one-way ANOVA followed by Bonferroni post-hoc testing. Differences between groups were considered to be statistically significant at *p < 0.05. All data are expressed as mean +/- SD and represent at least n = 3 independent sets of data.

Supplementary figures

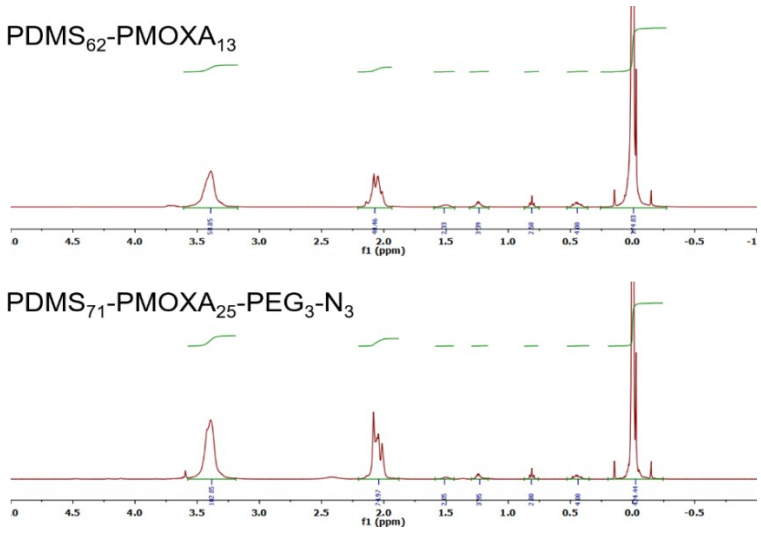

Figure S1. ^{1}H NMR spectra of $PDMS_{62}$-$PMOXA_{13}$ and $PDMS_{71}$-$PMOXA_{25}$-OEG_3-N_3 block copolymers in $CDCl_3$ without TMS recorded at room temperature.

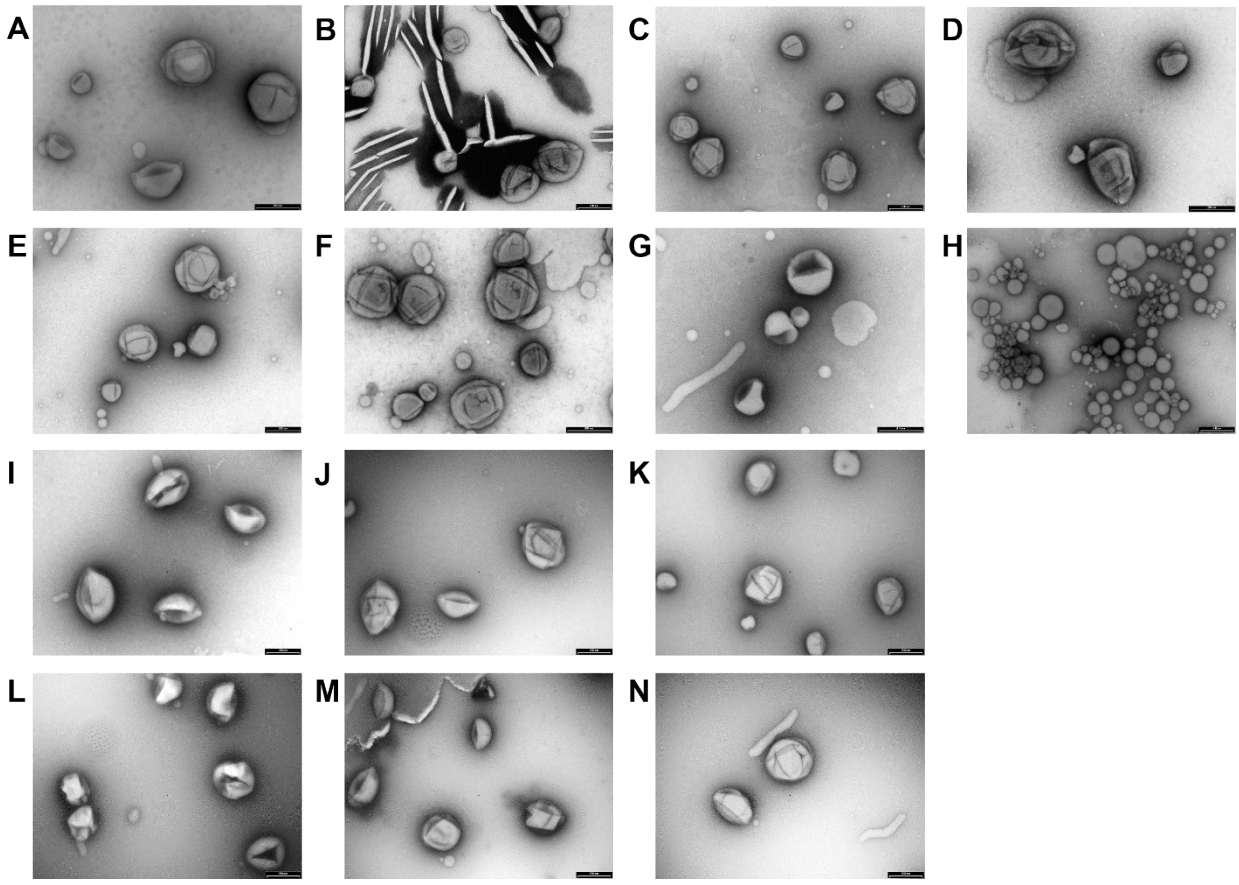

Figure S2. TEM micrographs of polymersomes and ssDNA-polymersomes. The polymersomes were assembled by $PDMS_{62}$-$PMOXA_{13}$ and $PDMS_{71}$-$PMOXA_{25}$-OEG_3-N_3 block copolymers in various molar ratios. Vesicular structures were observed for: (A) $PDMS_{62}$-$PMOXA_{13}$ alone and when $PDMS_{62}$-$PMOXA_{13}$ was mixed with: (B) 0.5 mol% (P0.5), (C) 1 mol% (P1), (D) 5 mol% (P5), (E) 10 mol% (P10) and (F) 20 mol% (P20) of $PDMS_{71}$-$PMOXA_{25}$-OEG_3-N_3. A mixture of vesicles along with worm-like micelles and spherical micelles was observed when: (G) 33 mol% of $PDMS_{71}$-$PMOXA_{25}$-OEG_3-N_3 was used (P33); (H) $PDMS_{71}$-$PMOXA_{25}$-OEG_3-N_3 alone assembled to spherical micelles. Addition of ssDNAa did not affect the polymersome architecture (I) P0.5-a, (J) P1-a, (K) P5-a, (L) P10-a, (M) P20-a, and (N) P33-a. The scale bar is 500 nm.

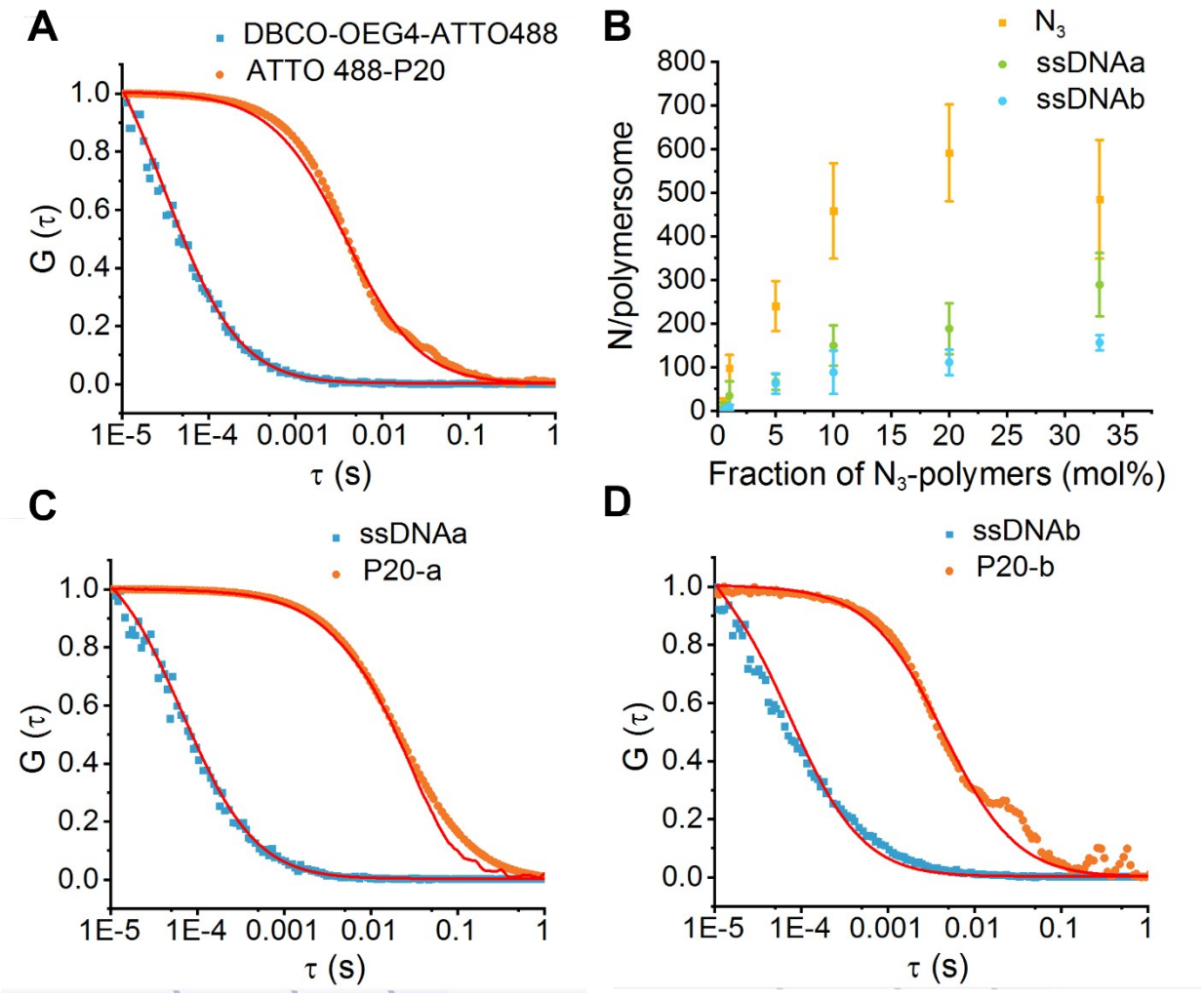

Figure S3. Quantification of available azide functional groups and ssDNA per polymersome via FCS. (A) Normalized FCS autocorrelation curves of DBCO-OEG4-ATTO 488 (blue) and P20 conjugated with DBCO-OEG4-ATTO 488 (orange) with their respective fits (red); (B) The number of azide groups (orange), ssDNAa (green) and ssDNAb (blue) per polymersome with various N_3 content; (C) Normalized FCS autocorrelation curves of ssDNAa-ATTO 488 (blue) and ssDNAa-ATTO 488 conjugating polymersomes with 20% azide-functionalized polymers (orange) together with their respective fits (red); (D) Normalized FCS autocorrelation curves of ssDNAb-cy5 (blue) and the ssDNAb-cy5 conjugating polymersomes (orange) together with their respective

fits (red). Series of 30 × 10 s were measured for each sample. Each point represents the average correlation coefficient G(τ) of 30 repeated measurements at a specific lag time τ.

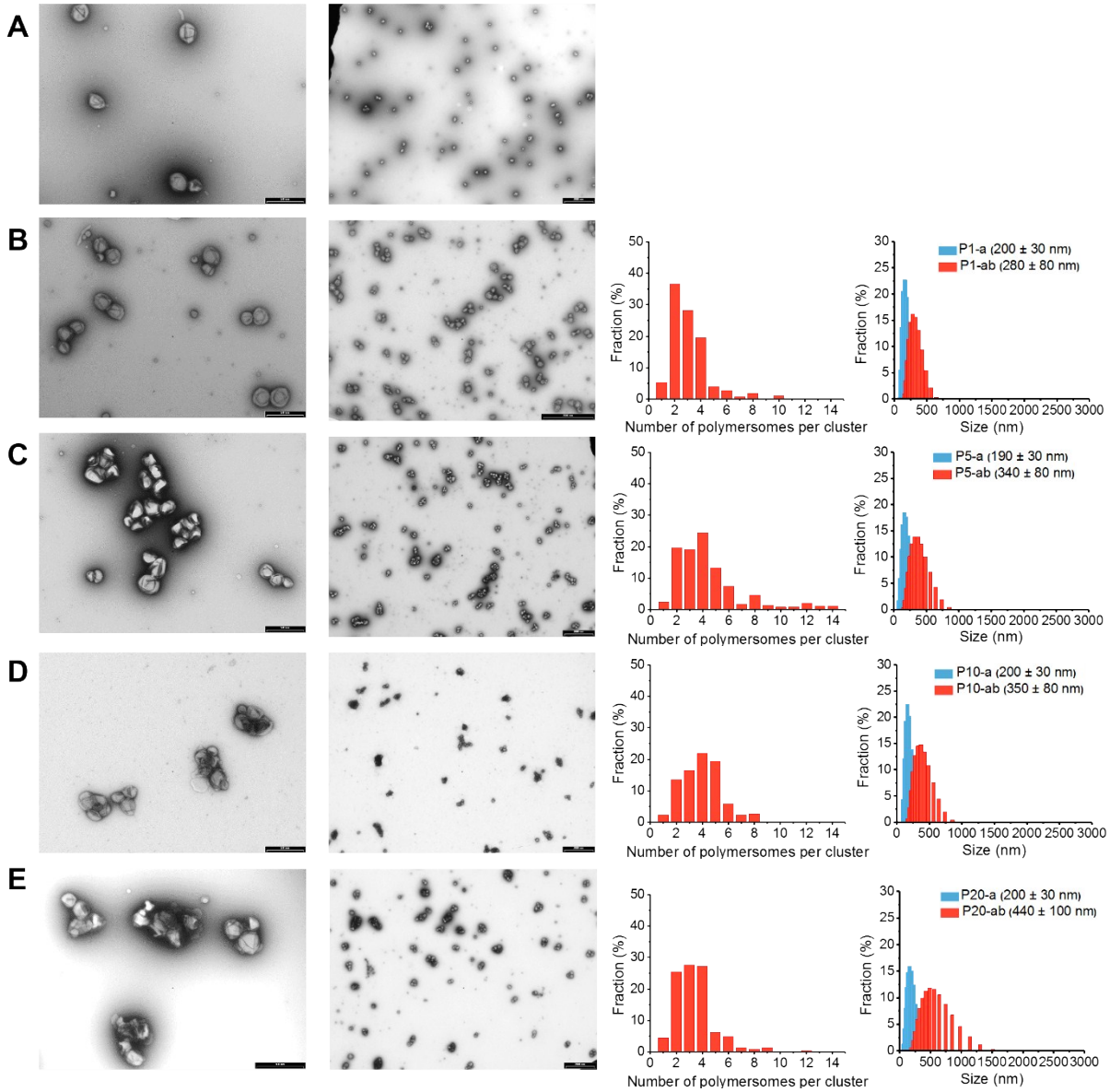

Figure S4. TEM and DLS characterization of DNA-linked polymersome clusters: (A) P0.5-ab, (B) P1-ab, (C) P5-ab, (D) P10-ab and (E) P20-ab*. Individual DNA-linked polymersome clusters are presented in zoomed and overall TEM micrographs with a scale bar of 500 nm (first column) and 2 µm, respectively (second column). 220 DNA-linked polymersome clusters from TEM

micrographs were used for the statistical analysis of the distribution of the number of polymersomes per cluster (third column). The distribution of the average apparent D_H obtained from DLS of: (blue) ssDNAa-polymersomes and (red) the corresponding DNA-linked polymersome clusters (fourth column) **.

*The data from Fig. 1d is presented here as supplementary Fig. 4e for completeness.

**The fraction of DNA-linked polymersome clusters composed of i polymersomes per cluster, f_i was calculated as:

$$f_i = \frac{iN_i}{\sum_i iN_i} 100\%$$

N_i represents the number of DNA-linked clusters composed of i polymersomes (including 1). The number size distribution of P1-a, P5-a, P10-a, and P20-a and the corresponding polymersome clusters was determined by DLS. Each point represents the average value of 3 measurements. As a low population of large clusters (composed of ≥ 6 polymersomes and over 500 nm in diameter) is present in the solution (see column 3), the intensity size distribution was not selected for the analysis because the intensity of scattering is proportional to D_H^6 (from Rayleigh approximation) and the fraction of large clusters will be over-represented. Number size distribution derived from intensity size distribution using Mie theory was used and provided the distribution of the number of polymersome clusters as function of the size.

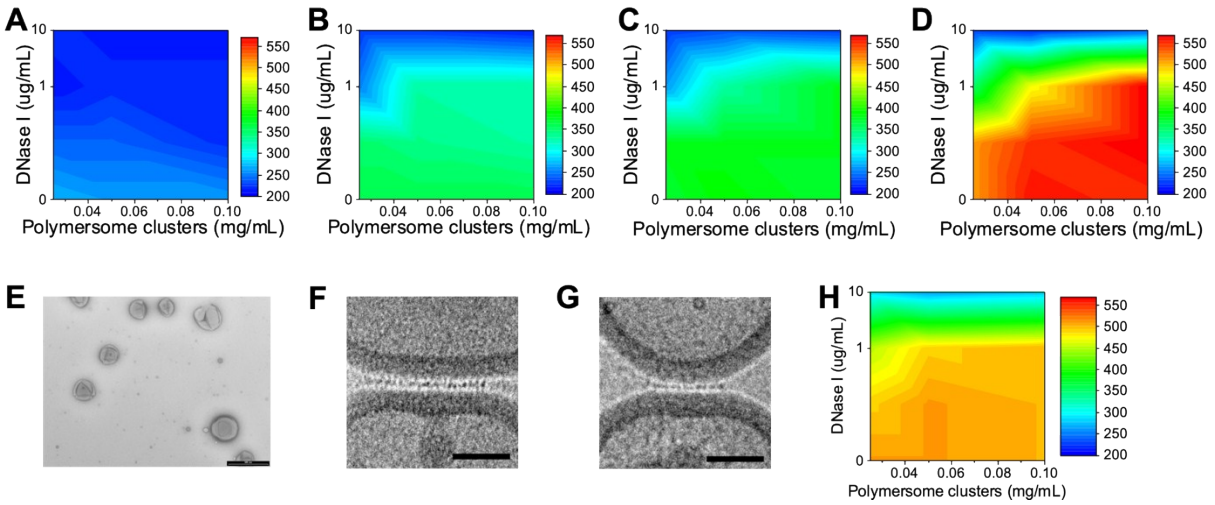

Figure S5. (A-D) Heat maps to determine the impact of nucleases on the stability of: P1-ab, P5-ab, P10-ab and P20-ab 22-bp DNA-linked polymersome clusters; distribution from 200 nm (blue) up to 550 nm (red) at specific DNase I and polymersome cluster concentrations (n = 3). The concentration of polymersome cluster was varied from 0.025 mg/mL to 0.1 mg/mL and the concentration of DNase I was varied from 0 to10 µg/mL. (E) TEM micrograph of P20-a and P20-b pretreated with 1 µg/mL DNase I at 37 ºC for 24 h. No clusters were formed after DNase I treatment. Scale bar = 500 nm (F-G) Cryo-TEM micrographs reveal the distance of DNA bridging area between DNA-linked polymersomes linked by 22-bp ssDNA and 11-bp ssDNA. Scale bar = 50 nm. (H) Heat map of polymersome clusters linked by 11-bp ssDNA with a size cluster distribution from 200 nm (blue) to 550 nm (red) at specific DNase I and polymersome cluster concentrations.

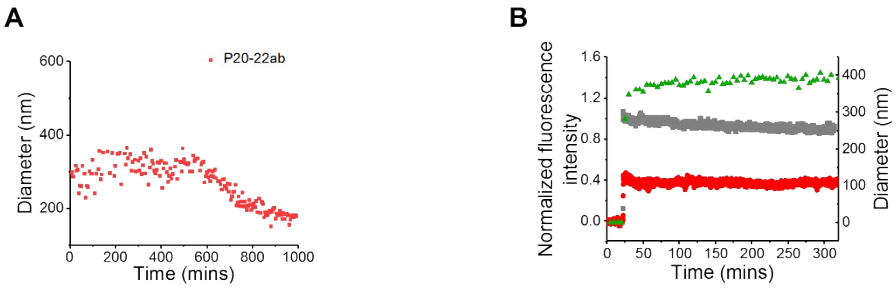

Characterization of polymersome clusters used for *in vitro* studies

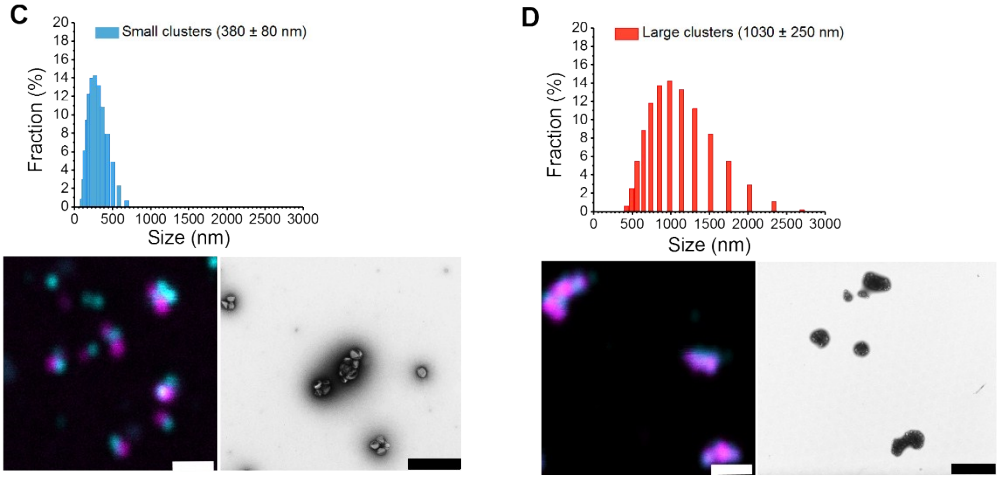

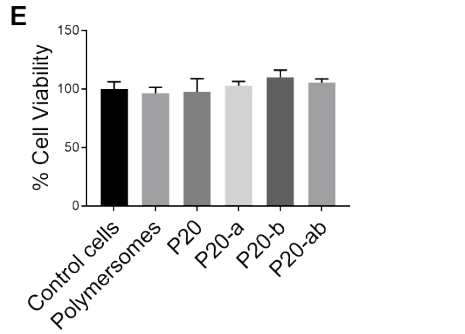

Characterization of polymersome clusters used for *in vivo* studies

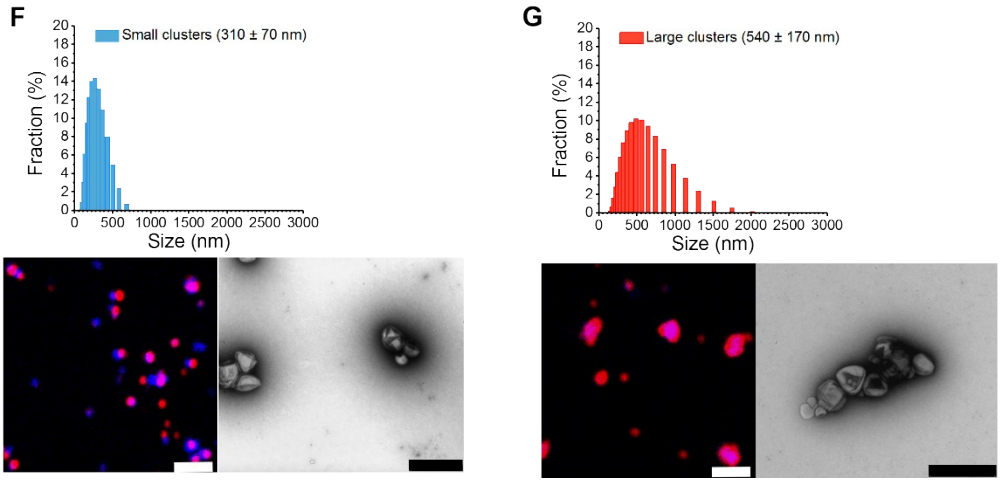

Figure S6. Stability and characterization of DNA-linked polymersome clusters for *in vitro* and *in vivo* studies. (A) Stability of P20-ab polymersome clusters linked by 22-bp ssDNA in cell medium with 10% FCS at 37 ˚C monitored by DLS. (B) FRET analysis confirming migration of ssDNA to the bridging area corresponding to zipped-polymersomes. The plots in gray and in red record the increase in florescence emission at 660 nm (λ_{ex} = 530 nm) resulting from the hybridization of excess free ssDNAa-Cy3 and P20-b-Cy3 to ssDNAa-Cy5 on P20. The change in size was monitored additionally by DLS (green). (C) Apparent diameter (number distribution), TEM and CLSM micrographs of small clusters for *in vitro* studies. Polymersomes for *in vitro* study represent: (cyan) ATTO-488-loaded P20-b (ATTO-488-P20-b) and (magenta) DY-633-loaded P20-a (DY-633-P20-a). The scale bars are: 2 μm for CLSM micrograph and 1 μm for TEM micrograph. (D) Apparent diameter (number distribution), TEM and CLSM micrographs of large clusters for *in vitro* studies. The scale bars are: 2 μm for CLSM micrograph and TEM micrograph. (E) MTS cell viability of HeLa cells incubated for 24h in presence of: polymersomes containing no azide functionalized polymer (Polymersomes), polymersomes with 20 mol% azide functionalized polymer (P20), ssDNAa/b polymersomes (P20-a and P20-b) and DNA-linked polymersome clusters with 400 nm average size (P20-ab). The polymersomes and polymersome assemblies do not exhibit a cytotoxic effect on the cells as compared to control untreated cells. (n = 4). (F) Apparent diameter (number distribution), TEM and CLSM micrographs of small clusters for *in vivo* studies. Polymersomes for *in vivo* study represent: (blue) DY-633-loaded P20-a (DY-633-P20-a), and (red) SRB-loaded P20-b (SRB-P20-b). The scale bars are: 2 μm for CLSM micrograph and 0.5 μm for TEM micrograph. (G) Apparent diameter (number distribution), TEM and CLSM micrographs of large clusters for *in vivo* studies. The scale bars are: 2 μm for CLSM micrograph and 0.5 μm for TEM micrograph.

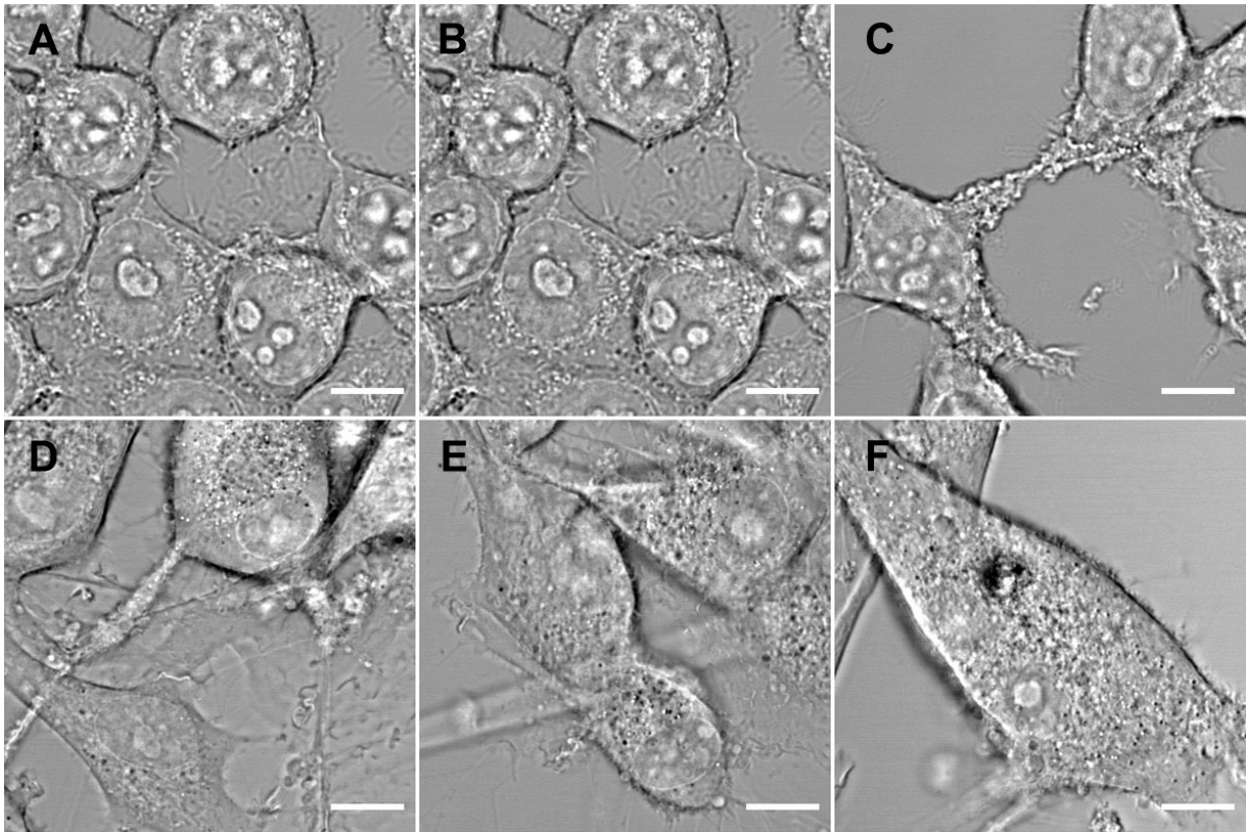

Figure S7. CLSM transmission channel micrographs showing cell morphology. (A) HEK293T cells incubated in presence of DY-633-P20-a, (B) HEK293T cells incubated in presence of small clusters (average size of 400 nm), and (C) HEK293T cells incubated in presence of large clusters (average size 1000 nm). (D) U87-MG cells incubated in presence of DY-633-P20-a, (E) U87-MG cells incubated in presence of small clusters (average size of 400 nm), (F) U87-MG cells incubated in presence of large clusters (average size 1000 nm). Scale bar 10 μm.

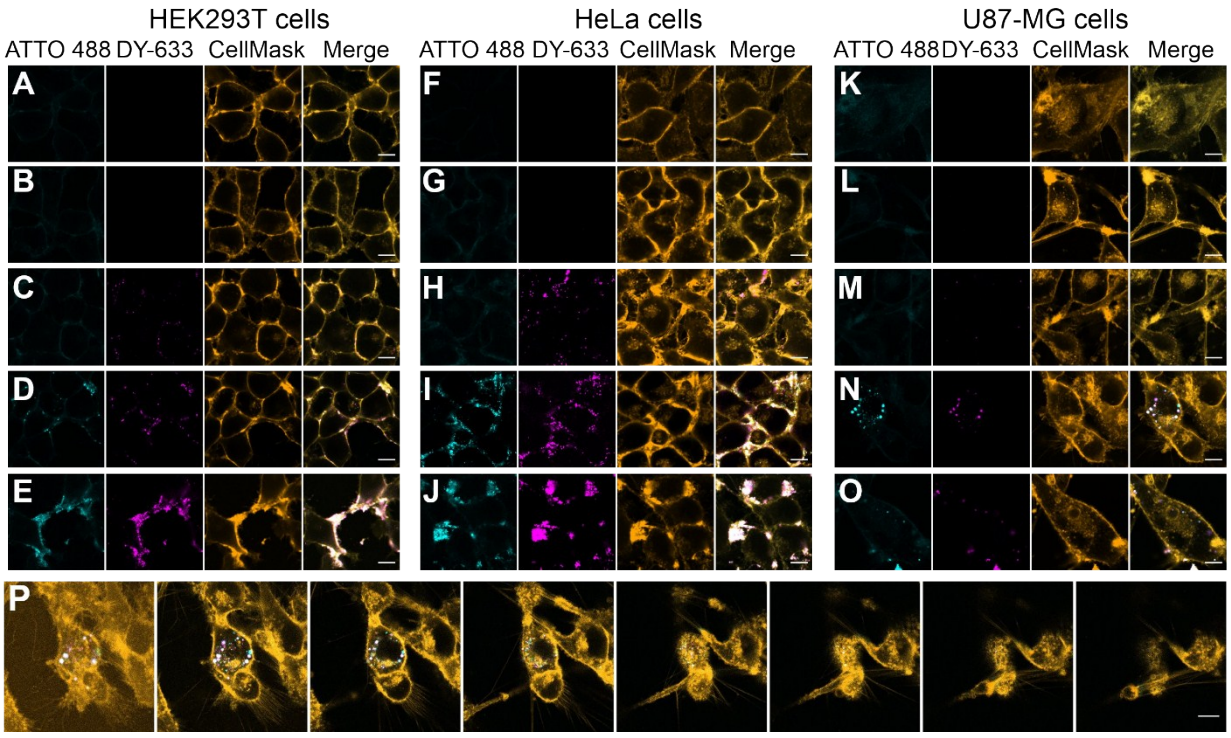

Figure S8. CLSM micrographs of DNA-linked polymersome cluster interactions with epithelial cells. (A) control HEK293T cells, (B) HEK293T cells incubated in presence of non-modified polymersomes, (C) HEK293T cells incubated in presence of DY-633-P20-a, (D) HEK293T cells incubated in presence of small clusters (average size of 400 nm), and (E) HEK293T cells incubated in presence of large clusters (average size 1000 nm). (F) Control HeLa cells, (G) HeLa cells incubated in presence of non-modified polymersomes, (H) HeLa cells incubated in presence of DY-633-P20-a, (I) HeLa cells incubated in presence of small clusters (average size of 400 nm) and (J) HeLa cells incubated in presence of large clusters (average size 1000 nm). (K) Control U87-MG cells, (L) U87-MG cells incubated in presence of non-modified polymersomes, (M) U87-MG cells incubated in presence of DY-633-P20-a, (N) U87-MG cells incubated in presence of small clusters (average size of 400 nm), (O) U87-MG cells incubated in presence of large clusters (average size 1000 nm) and (P) z-stack of internalized 400 nm small clusters in U87-MG cells. Cells were stained with Cell Mask Orange before imaging. Scale bar 10 µm.

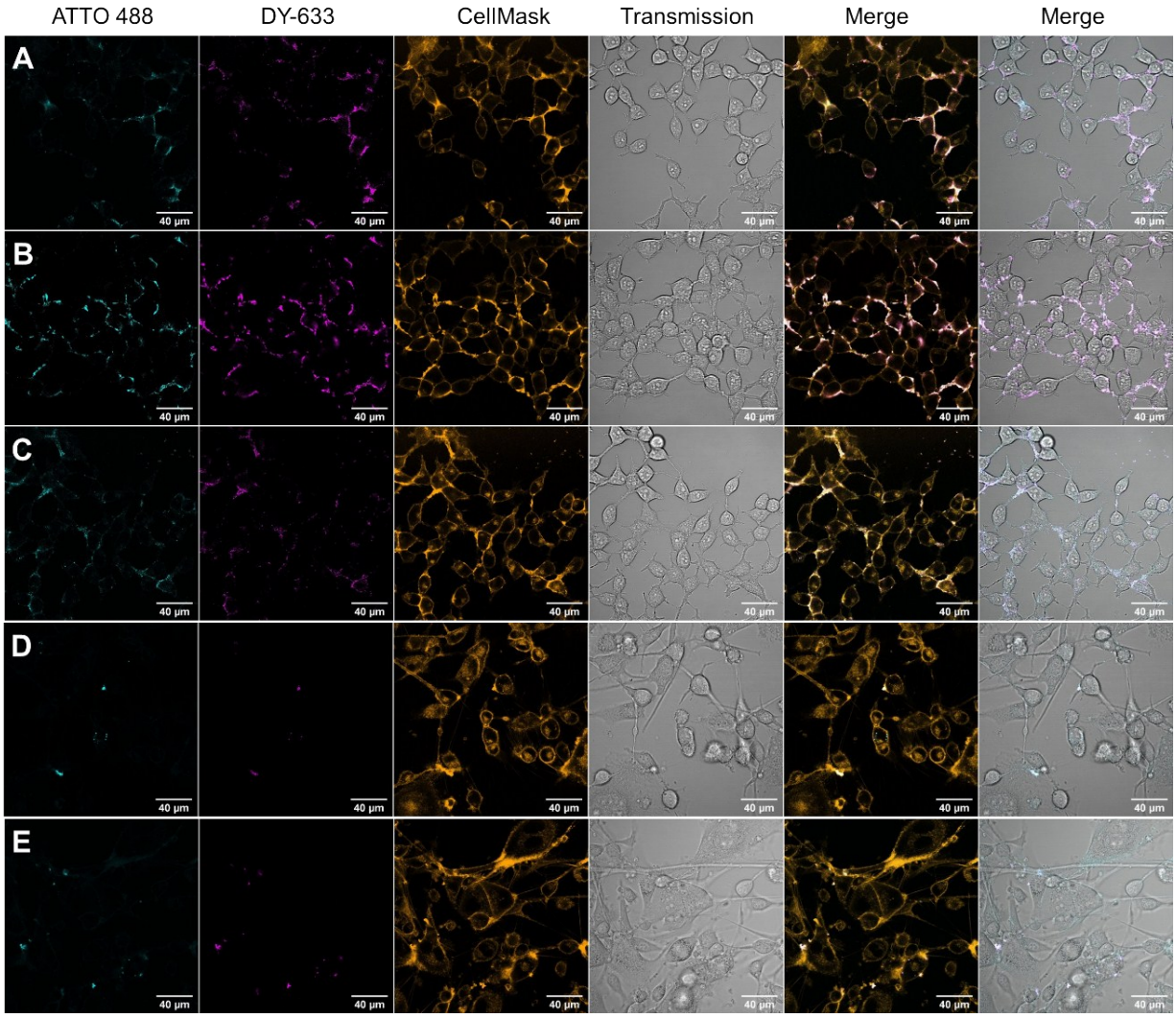

Figure S9. CLSM micrographs of DNA-linked polymersome cluster interactions with epithelial cells. (A-C) HEK293T cells incubated in presence of clusters showing large coverage of the cell surface and limited uptake. (D-E) U87-MG cells incubated in presence of clusters showing limited uptake and limited binding to the cell surface. Cells were stained with Cell Mask Orange before imaging. Scale bar 40 µm.

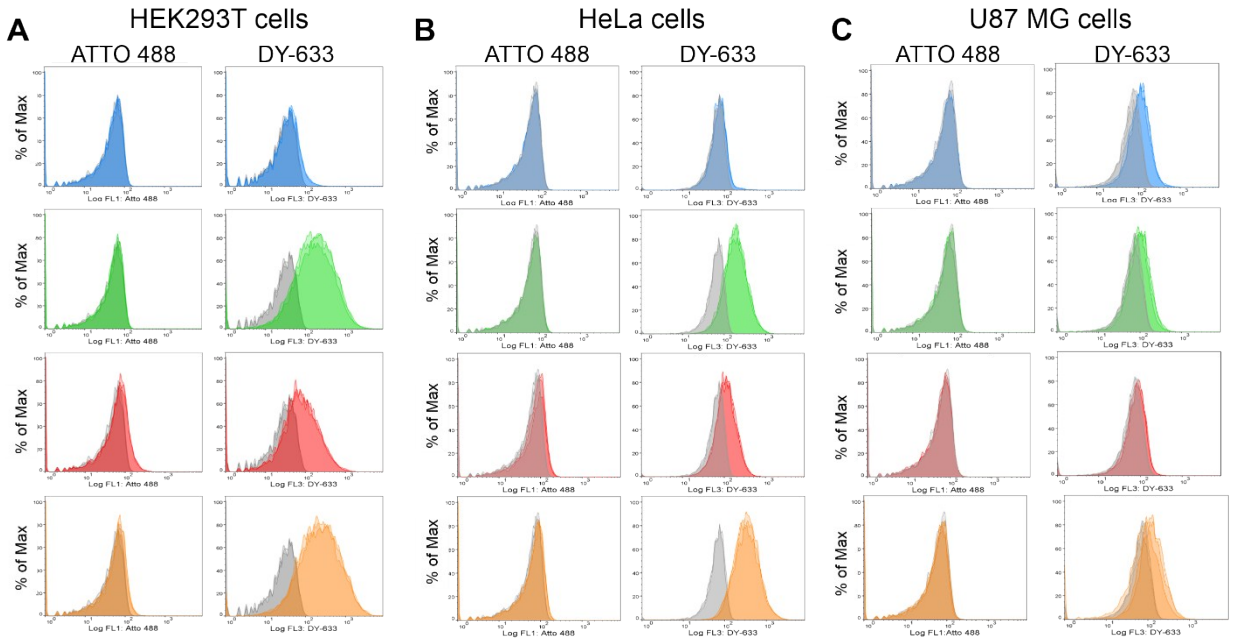

Figure S10. Flow cytometry analysis of: (A) HEK293T incubated in presence of DY-633-loaded unmodified polymersomes (blue), DY-633-P20-a polymersomes (green), small DNA-linked polymersome clusters (average size 400 nm) (red), and large DNA-linked polymersome clusters (average size 1000 nm) (yellow). (B) HeLa incubated in presence of: DY-633-loaded unmodified polymersomes (blue), DY-633-P20-a polymersomes (green), small DNA-linked polymersome clusters (average size 400 nm) (red), and large DNA-linked polymersome clusters (average size 1000 nm) (yellow). (C) U87 MG cells incubated in presence of: DY-633-loaded unmodified polymersomes (blue), DY-633-P20-a polymersomes (green), small DNA-linked polymersome clusters (average size 400 nm) (red), and large DNA-linked polymersome clusters (average size 1000 nm) (yellow). Control: untreated cells shown in grey in all measurements (n = 3). A shift in fluorescence can be observed for cells incubated in the presence of either ssDNA-P20-a, 400 nm small clusters and 1000 nm large clusters. The encapsulation efficiency of DY-633 in polymersomes is 24.7 % and for ATTO 488 is 10.4 %, therefore the fluorescence shifts in the DY-633 channel are larger than for the ATTO 488 channel. Shifts are observed for cells treated with

DY-633-P20-a polymersomes because for the ssDNA polymersomes the entire population contains only DY-633 dye, while for the clusters, statistically, half of the polymersomes contain DY-633 and half ATTO 488.

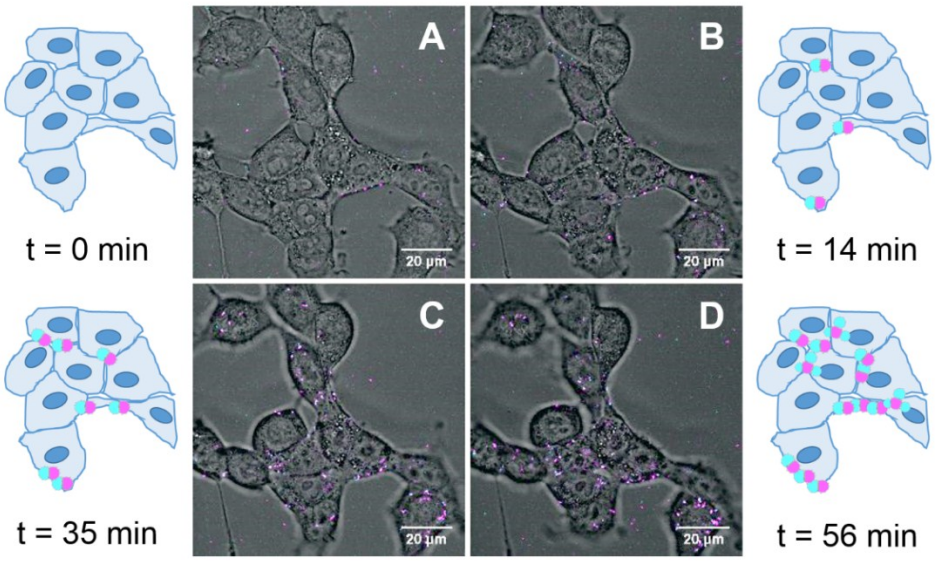

Figure S11. Attachment of 22bp DNA-linked polymersome clusters (average size 400 nm) to cell surface of HEK293T cells at (A) t = 0 min, (B) t = 14 min, (C) t = 35 min and (D) t = 56 min.

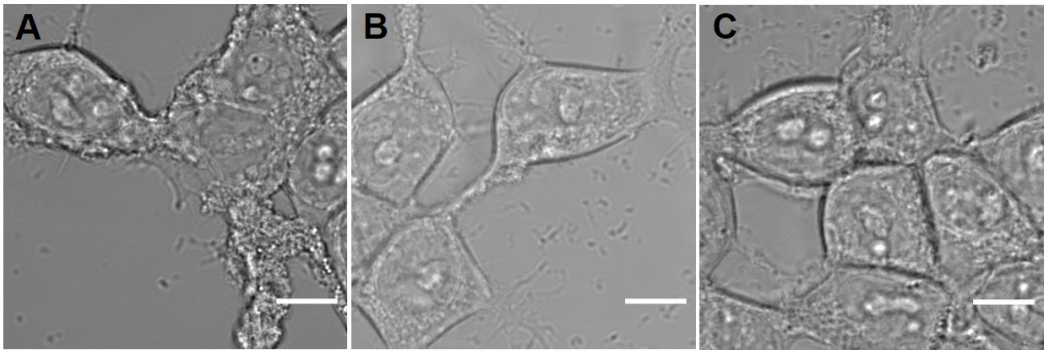

Figure S12. CLSM transmission channel micrographs showing cell morphology. Cells incubated in presence of large DNA-linked polymersome clusters (average size 1000 nm) and increasing concentration of scavenger receptor inhibitor Fucoidan at (A) 0 µg/mL, (B) 10 µg/mL and (C) 50 µg/mL. Scale bar 10 µm.

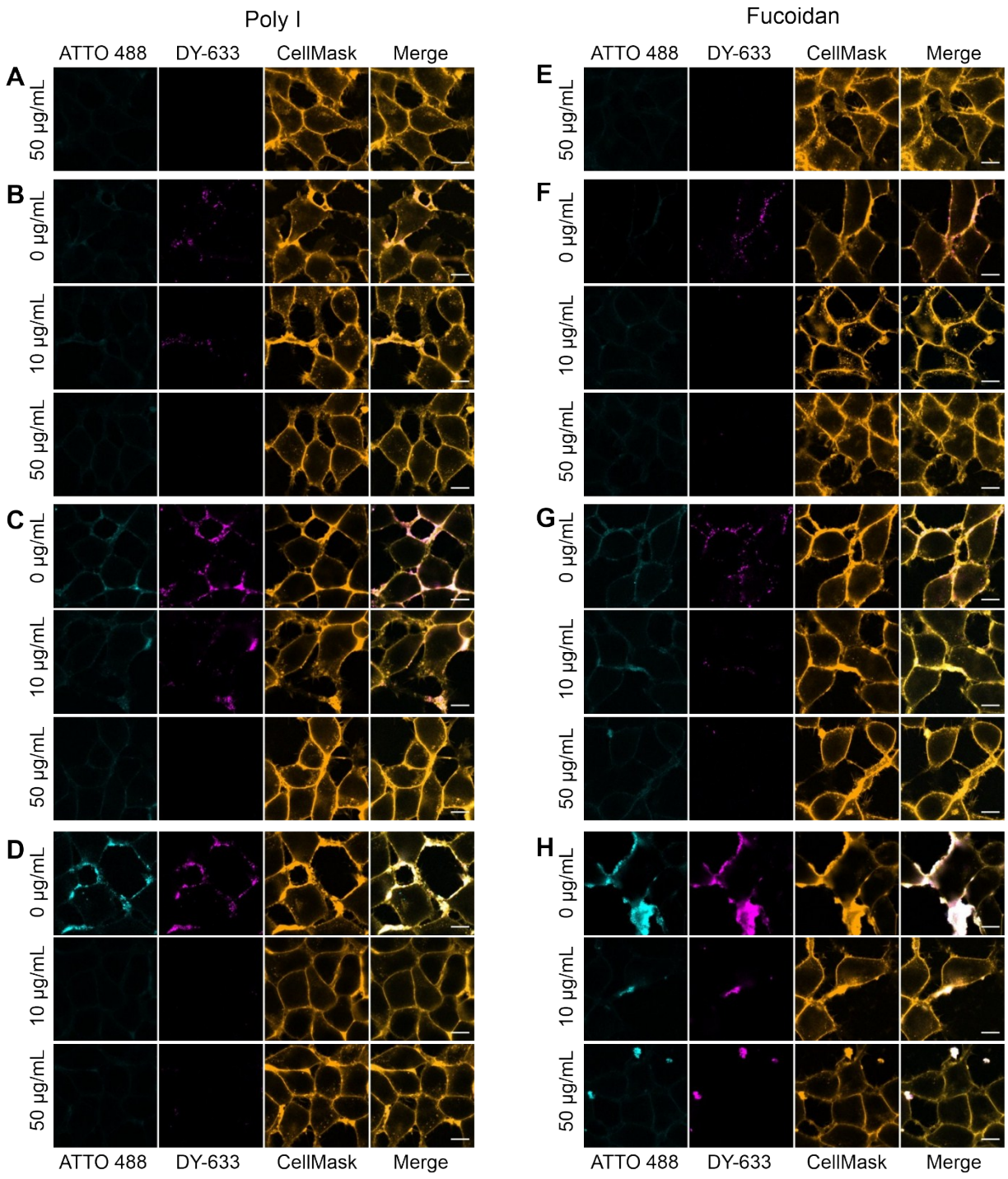

Figure S13. CLSM micrographs of HEK293T cells incubated in presence of: (A) 50 µg/mL PolyI only; (B) DY-633-P20-a polymersomes and increasing concentration of scavenger receptor inhibitor PolyI at 0, 10 and 50 µg/mL; (C) small DNA-linked polymersome clusters (average size

400 nm) and increasing concentration of scavenger receptor inhibitor PolyI at 0, 10 and 50 μg/mL; (D) large DNA-linked polymersome clusters (average size 1000 nm) and increasing concentration of scavenger receptor inhibitor PolyI at 0, 10 and 50 μg/mL; (E) 50 μg/mL Fucoidan only; (F) DY-633-P20-a polymersomes and increasing concentration of scavenger receptor inhibitor Fucoidan at 0, 10 and 50 μg/mL; (G) small DNA-linked polymersome clusters (average size 400 nm) and increasing concentration of scavenger receptor inhibitor Fucoidan at 0, 10 and 50 μg/mL; (H) large DNA-linked polymersome clusters (average size 1000 nm) and increasing concentration of scavenger receptor inhibitor Fucoidan at 0, 10 and 50 μg/mL. Faint fluorescent signal visible at high concentrations of the inhibitors in the ATTO 488 channel is a result of autofluorescence. Scale bar 10 μm.

Supplementary Tables

Table S1. Number average molecular weight (Mn) and polydispersity index (PDI) of $PDMS_{62}$-$PMOXA_{13}$ and $PDMS_{71}$-$PMOXA_{25}$-OEG_3-N_3.

Composition	Mn[a] (kg/mol)	Mn[b] (kg/mol)	PDI[b]
$PDMS_{62}$-$PMOXA_{13}$	5.8	5.8	1.3
$PDMS_{71}$-$PMOXA_{25}$-OEG_3-N_3	7.7	6.4	1.2

[a] Mn was determined by ^1H NMR end group analysis.

[b] Mn and PDI was determined by GPC.

Table S2. Apparent D_H (mean ± s.e.m) of azide-functionalized polymersomes (P), P-a and P-b analyzed by DLS.

polymersomes	D_H of P (nm)	D_H of P-a (nm)	D_H of P-b (nm)
P0			
P0.5	210 ± 30	210 ± 30	200 ± 30
P1	190 ± 30	200 ± 30	190 ± 30
P5	200 ± 30	190 ± 30	210 ± 30
P10	200 ± 30	200 ± 30	200 ± 30
P20	200 ± 30	200 ± 30	190 ± 30
P33	200 ± 30	200 ± 30	200 ± 30

Table S3. DNA surface density (σ, mean ± s.d.) on polymersomes.

ssDNAa-polymersomes	σ (× 10^{-5} nm^2)	ssDNAb-polymersomes	σ (× 10^{-5} nm^2)
P0.5-a	7 ± 8	P0.5-b	1 ± 1
P1-a	27 ± 26	P1-b	6 ± 4
P5-a	51 ± 14	P5-b	48 ± 17
P10-a	115 ± 35	P10-b	67 ± 38
P20-a	144 ± 44	P20-b	86 ± 22
P33-a	222 ± 56	P33-b	120 ± 14

An average apparent D_H of 200 nm for polymersome was used, resulting in an average surface area of 1.3×10^5 nm^2. DNA density on polymersome's surface was calculated by dividing the number of ssDNA per polymersome by the average surface area of polymersome.

Table S4. ζ potential of single ssDNA-polymersomes and small and large clusters in PBS and cell medium with serum. All results present as mean ± s.e.m. of 3 experiments.

	ζ potential in PBS (mV)	ζ potential in cell medium with serum (mV)
DY-633-P20-a	- 11.00 ± 0.04	-8.95 ± 0.05
ATTO 488-P20-b	- 10.60 ± 0.02	-9.54 ± 0.08
small clusters	- 5.47 ± 0.02	-6.60 ± 0.01
DY-633-P20-a-L[a]	-17.40 ± 0.05	-12.90 ± 0.05
ATTO 488-P20-b-L	-18.2 ± 0.08	-13.23 ± 0.03
Large clusters	- 8.97 ± 0.04	-10.93 ± 0.02

[a] DY-633-P20-a-L and ATTO 488-P20-b-L represent the ssDNA-polymersomes for the formation of large clusters. The preparation of DY-633-P20-a-L and ATTO 488-P20-b-L is described in the Method in details.